1989 Wire Chamber Conference
Vienna, Austria
February 13-17, 1989

CONF-890231--7

BNL-42683

M.W.P.C. with highly segmented cathode pad readout

BNL--42683

DE89 012672

R. Debbe, J. Fischer, D. Lissauer, T. Ludlam,
D. Makowiecki, V. Radeka, S. Rescia, G. C. Smith, D. Stephani, B. Yu
Brookhaven National Laboratory
Upton N.Y. 11973 *

1. Introduction

Experiments being conducted with high energy heavy ion beams at Brookhaven National Laboratory and at CERN have shown the importance of developing position sensitive detectors capable of handling events with high multiplicity in environments of high track density as will also be the case in future high luminosity colliders like SSC and RHIC. In addition these detectors are required to have a dynamic range wide enough to detect minimum ionizing particles and heavy ions like oxygen or silicon, see Ref 1.

We present here a description of work being done on a prototype of such a detector at BNL. Results from a similar counter are also presented in this Conference. (Ref. 2). The "pad chamber" is a detector with a cathode area subdivided into a very large number of pixel-like elements such that a charged particle traversing the detector at normal incidence leaves an induced charge on a few localized pads. The pads are interconnected by a resistive strip, and readout amplifiers are connected to the resistive strip at appropiate, carefully determined spacings. (see Fig. 1). The pattern of tracks in a multi-hit event is easily recognized, and a centroid-finding readout system allows position determination to a small fraction of the basic cell size.

The present paper is organized in the following way: Section 2 describes simulations carried out before the construction of our prototype in order to fix some of its parameters and to evaluate how well this detector performs in high multiplicity events. In section 3 we report the techniques used for construction. Section 4 is a description of tests conducted on the chamber with a collimated X-ray beam with energy equal to 5.4 keV.

* This research was supported by the U. S. Department of Energy, Division of Basic Energy Sciences under contract No. DE-AC02-76CH00016.

2. Chamber design

This detector works as a multi-wire proportional chamber. Charged particles passing through the active gas volume leave clusters of electron-ion pairs along their trajectory. The electric field of the chamber is configured in such a way as to define independent regions around the anode wires. All clusters formed inside one region drift to a single anode wire, and there, an avalanche process multiplies the charge. The localized ion cloud resulting from the electron avalanche induces charge distributions in all neighbouring conductors.

A square cell with dimension 4x4 mm was selected (see Figure 1 a and b) and the field was simulated using the CERN program GARFIELD (Ref 3). The sense wires were set at positive potential with a value around one thousand volts. The field wires define the boundaries of cells. The voltages were chosen in order to obtain electric fields at the surface of the sense wire with magnitudes in the order of 200 $\frac{kV}{cm}$, thus producing avalanches with gains of the order of 10^4.

For our particular design we estimate that 20% of the charge collected on the anode is induced on the cathode plane. The charge induced on this plane was evaluated. The insert in Figure 1b shows the shape of this distribution as is given by the GARFIELD program. Strips of copper that we call guard strips were placed between pad rows to minimize the charge induced at neighboring rows (crosstalk). A compromise on the size of pads and guard strip has to be found; the bigger the pad size the more charge is collected, but the crosstalk is also increased. The number of readouts under the same anode wire has to be selected in such a way as to maximize the position resolution of the detector. From [Ref 4] we know that the position resolution depends on the capacitance of the electrodes, the number of readouts and the charge collected on the cathode in the following way:

$$fwhm\ \alpha\ \frac{C^{1/2}l}{Q_s N^{\frac{3}{2}}}$$

where C is the capacitance of the row of pads under one anode wire, Q_s the charge collected on the cathode plane, N the number of readouts, and l the length of the detector.

With 20% of the charge collected on the anode expected to be induced on the pad row, and a value of $C_{DS} = C/N$ around 3 pF (C_{DS} being the capacitance of one readout) we estimated the number of readouts necessary to obtain position resolution of the order of $100\mu m$ for a minimum ionizing particle to be around 20 for a detector 20 cm long.

The guard strips were placed between pad rows in order to reduce the charge induced on pads underneath wires next to the one where the avalanche ocurred. Without the strips,

the ratio of charge between pad rows is equal to 16%. Strips 1 mm wide reduce this ratio to 6%. Wider guard strips reduce the amount of charge collected under the main wire. We decided, therefore, to build the prototype with guard strips 1 mm wide, and pad size 0.6 mm. along the wire and 2 mm across it. The pad pitch, along the wire direction, is 1 mm and every tenth pad is read out.

Once the dimensions of the readout plane were selected, a simulation of the chamber proceded in the following way: A determined number of particles with $\beta = 1$ and normal incidence passed through the active volume of the detector. The distance between electron clusters produced by ionization in the gas (90% Argon 10% Methane) is extracted from a Poisson distribution and the number of electron-ion pairs in each cluster was obtained using a modified Landau distribution. The average number of clusters is equal to 10 with each cluster having on the average two electron-ion pairs. Diffusion of the electrons during the drift to the sense wires was also included, but doesn't have a significant effect in our simulations. The incidence of particles to this detector is expected to be, most of the time, normal to the chamber and in very few cases where the particles pass very near the boundary of the cells some of the clusters will drift to a neighboring cell. A second program was developed to study events with high multiplicity. In this program all electrons produced by the simulated tracks are assumed to drift to well localized points on the sense wires. The charge produced by the avalanche induces a charge distribution with almost circular symmetry on the cathode plane. The charge collected on each pad is divided linearly between the nearest readouts and an output for that event is produced. Figure 2 shows the amount of charge in each one of the readouts for one simulated event with 19 incident tracks in the 10 x 20 cm^2 active area. Our studies show that such a detector will have good efficiency for reconstructing events with this level of track density.

3. Construction.

Figure 3a is a cross section of the chamber and shows the location of anode and field wires, the two cathodes and the different layers that support the pad readout. Figure 3b shows the complete structure of the chamber. The wire plane was placed 2 mm above the pad plane, and an aluminized Mylar foil with a thickness of 12.5μm constitutes the second cathode plane, 4 mm away from the pad plane. The active volume had a flow of P10 gas (90% Argon 10% Methane). Positive high voltage was applied to the anode wires and the field wires were placed at one hundred volts of negative potential.

One of the most challenging parts of this project has been the manufacture of the cathode plane supporting the pad readout system. An important constraint on detectors

of this type is the mass they present to the particles being detected. We require that the total thickness be less than 0.01 radiation length. For the construction of this prototype a multi-layer board was built on sheets of fiber glass laminate (G10) $125\mu m$ thick. On the first layer the pad rows and guard strips were etched on copper sheet with a thickness of $5\mu m$. The second layer is a ground plane to reduce crosstalk to other channels that have their connection leads nearby. On the third layer the connection leads were etched in strips of copper with the same thickness as the pads and $200\mu m$ wide. (See figure 4). The connection between pads and readout leads is made with plated through holes. These layers were then pressed together. The total thickness of this assembly is $825\mu m$. The following layers (4-6) carry the voltage for the preamplifiers and a second ground plane.

The flatness of the cathode plane is important in order to keep the gain of the chamber constant throughout the active area. The relative change in gain, A, is related to the relative variations in the cathode anode separation, d, by the following approximate relation: Ref 5

$$\frac{\delta A}{A} \alpha \, 12 \frac{\delta d}{d}$$

Layers 4 to 6 have the active area cut out, with a reinforcement applied by glueing under pressure a plane 3.8 mm thick of HEXCELL fiberglass reinforced polymide honeycomb. With this reinforcement the thickness of the chamber remains 0.6 % radiation length and an excellent flatness was achieved resulting in measured gain variations of the order of $\pm 3\%$ over the active area of the chamber.

The charge division is done by a layer of resistive polymer which is deposited over the pad rows with a silk screening technique. The resistance between pads obtained after deposition have an average value of $8K\Omega$. In the future we plan to trim the resistive layer in order to make all resistances equal to within 2%.

Table 1 has the measured effective gains of our system for different values of anode and field wires. The measurement was done comparing the output of the amplification chain when a known amount of charge was injected to the preamplifier input, to that obtained with a source of Fe^{55} (5.9 keV X-ray source). The integration time for this measurement was set at 200 nsec.

Anode wires volts	Field wires	Gain of the chamber	
1050	-100	4000	
1100	0	5600	
1100	-100	7200	
1150	-100	14600	
1200	-100	28000	
1250	0	40000	
1250	-100	53000	

Figure 5 presents the output of the shaping amplifier for signals summed from all anode wires.

The amplification chain of our system consists of a charge sensitive preamplifier IO-456-4 with an input capacitance of about 4 pF. (The measured capacitance of ten pads to ground is equal to 2.5 pF.) This amplifier drives 6 feet of 110Ω twisted-pair cable to isolating transformers. A 50 ft shielded twisted-pair cable connects the transformer to a shaping amplifier with bipolar response function and 200 nsec shaping time.

Measurements were carried out by feeding the output of the shaping amplifiers to Camac and Fastbus ADC's. Some additional measurements were performed by analysis of the preamplifier output with an accurate centroid finding method (see Ref 4).

4. Testing of the chamber

Two calibration systems were built into the prototype detector. A strip 2.5 mm wide was etched on the first ground plane $380\mu m$ away from the leads connecting the pads to the preamplifiers. We also provided access to the anode wires in order to induce charge directly to the pads. The noise in the electronics chain was measured by inducing known amounts of charge on the calibration strip and it is found to be equivalent to 1500 electrons.

We have also made tests with a collimated beam of 5.4 keV X-rays with a cross section of $15\mu m$ by 0.5 mm. The beam entered normal to the chamber. The center of gravity of the charge collected in each readout was then calculated. The distribution of centroids for different positions of the incident beam is shown in Figure 6 . These distributions have standard deviations that range from 120 to $150\mu m$. The anode charge, Q_A, for these measurements was 0.3 pC (as determined in 200 nsec), which is the normal operating condition for the chamber in the particle beam experiment. The behavior of position resolution versus anode charge in any one location of the detector followed the standard pattern: for Q_A up to about 0.2 pC, the resolution improved according to a $\frac{1}{Q_A}$ relationship, since electronic noise was the only significant perturbing factor, while above 0.2 pC

position resolution improved progressively less quickly than $\frac{1}{Q_A}$ because of the influence of phenomena such as electron range and diffusion. A minimum value of about 70 μm RMS was attained for Q_A= 1.3 pC, and higher charge levels caused progressive deterioration in resolution because of spreading of the avalanche along the anode wire. The normal operating condition outlined above provided a gas gain significantly below that which causes avalanche spreading, but still yielded acceptable position resolution.

Another important parameter of the detector is position linearity. A convenient measure of this is the differential nonlinearity, which can be obtained from a spectrum of uniform irradiation. We have made an initial measurement of differential nonlinearity by carrying out a uniform irradiation response (UIR), with 5.4 keV X-rays, along a section of the anode wire. The preamplifier signals were fed to a special centroid finding system (see REF 4) and the resulting position signals analysed with a pulse height analyser. (The main reason for using this system, as opposed to the ADC's was to allow adequate counting statistics to be obtained) Figure 7a shows the UIR across eight readout pads, or nodes, of one pad row. The positions of the readout pads, separated by 1 cm, correspond to the tick marks on the abscissa. Differential nonlinearity is better than ±6%. Integration of the number of counts in each channel of the UIR allows us to evaluate the integral nonlinearity. The absolute position error derived by this method from the UIR is shown in Figure 7b, which shows that the maximum position error is $\pm 60 \mu m$.

We also studied the charge sharing from one pad row to the next. In order to do that we used the collimated beam of X-rays, $15 \mu m$ wide, and scanned the chamber from one cell boundary to the next. The beam was placed in such a way as to have the maximum signal on one of the readouts. The signal from the main anode wire and its neighbor were recorded as well as signals from the three pads directly underneath the main anode, and two more pads on the rows directly above and below.

Figure 8 shows the ratios of charge shared to the next pad row as a function of the vertical position of the X-ray beam. The pad row associated with the anode wire below the main wire receives an average 1.5 to 2% of the charge and the pad row associated with the anode wire above barely receives 1% of the charge. The asymmetry can be explained by the main wire not being placed exactly in the center of the pad row. And the overall low ratios indicate, as does figure 8, that the charge distribution is narrower than the assumed distributions used for the simulations. Figure 9 shows the amount of charge collected for different positions of the collimated beam. As can be seen in this figure, the charge is completely collected on one anode wire for more than 96% of the cell size.

5. Acknowledgements

A detector of this nature involves many areas of technology and implies the assistance of several individuals. In particular we would like to acknowledge useful discussions with Craig Woody during the testing of the detector and help from Tom Willis with data taking. The production of the multi-layer cathode pad plane was carefully done by Tony De Libero and Ron Angona, and a large part of the rest of the detector was constructed by Bob Chanda. We acknoledge the help of Lee Rogers with the testing of the shaping amplifiers.

References

1 T. Ludlam, P. D. Bond, R. Debbe, V. Radeka BNL E802 note (Oct. 1985).

2 B. Sellden et al. Proceedings of this Conference.

3 Rob Veenhof NA34 experiment CERN. Private communication.

4 V. Radeka and R. Boie NIM 178 (1980) 543-554

5 F. Sauli CERN 77-09 (1977)

Figure captions

Fig. 1a Detail of the detector showing all separate components.

Fig. 1b Cross section of the detector (AW: anode wire, FW: field shaping wire). The distribution of the induced charge is also shown.

Fig. 2 Amounts of charge on all readouts for a simulated event with 19 tracks.

Fig. 3a A view of the detector indicating all layers of the cathode plane.

Fig. 3b Wire frame and foils.

Fig. 4 A section of the art work for the connection leads on the cathode plane.

Fig. 5 Signal obtained at the output of the shaping amplifier from all anode wires when the chambers is irradiated with an Fe^{55} source

Fig. 6 Distribution of calculated centroids for four different positions of the collimated X-ray beam.

Fig. 7a Distribution of calculated centroids of charge for uniform illumination of the chamber with X-rays of 5.4 keV.

Fig. 7b Integrated nonlinearity obtained by adding the contents of all channels in figure 7a and subtracting the results from a straight line that would correspond to a perfectly linear counter.

Fig. 8 Ratios of charge shared to next pad rows as a function of the beam position for vertical scans across one cell.

Fig. 9 Charge collected on one anode wire versus vertical source position.

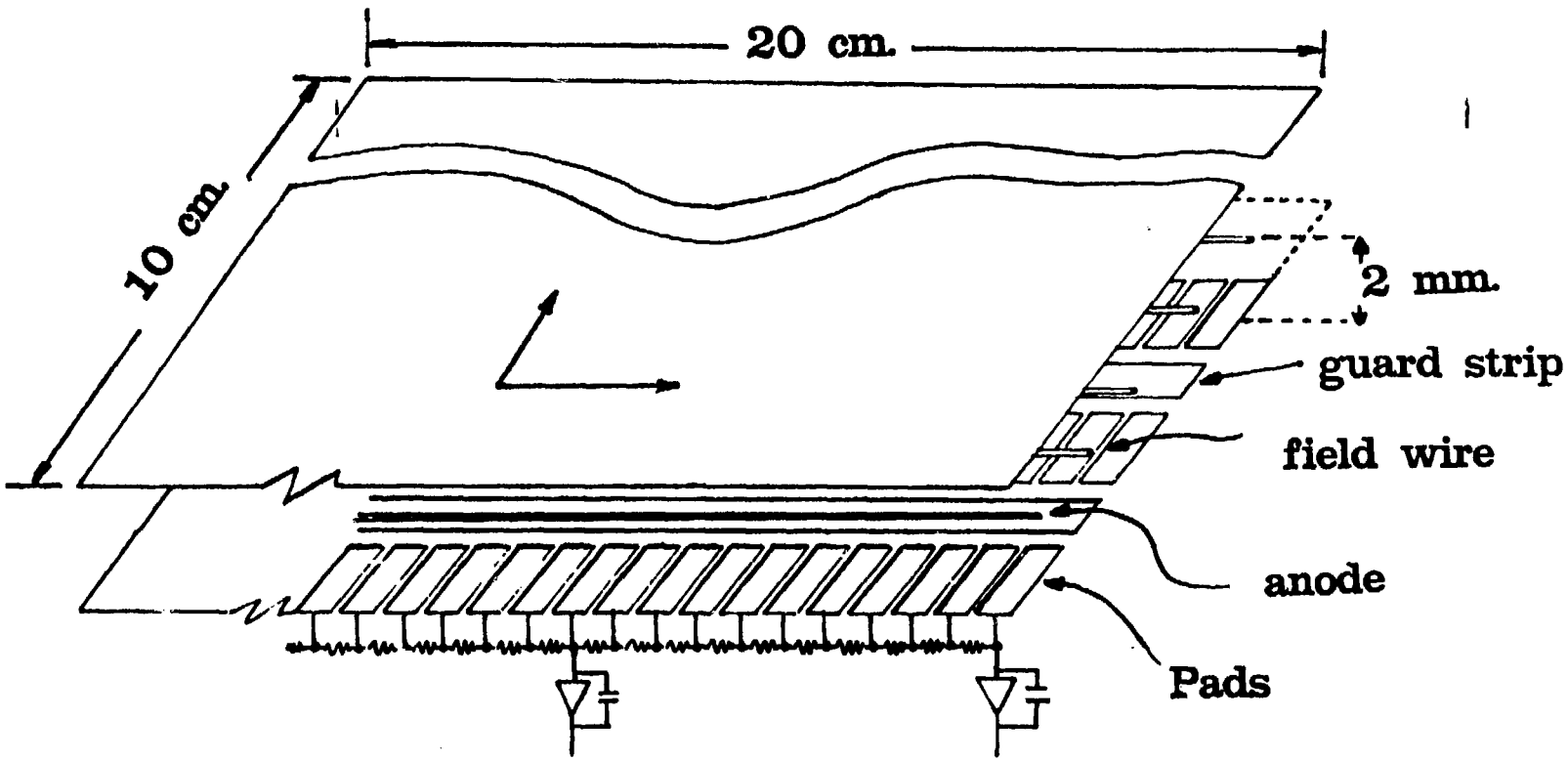

Figure 1a

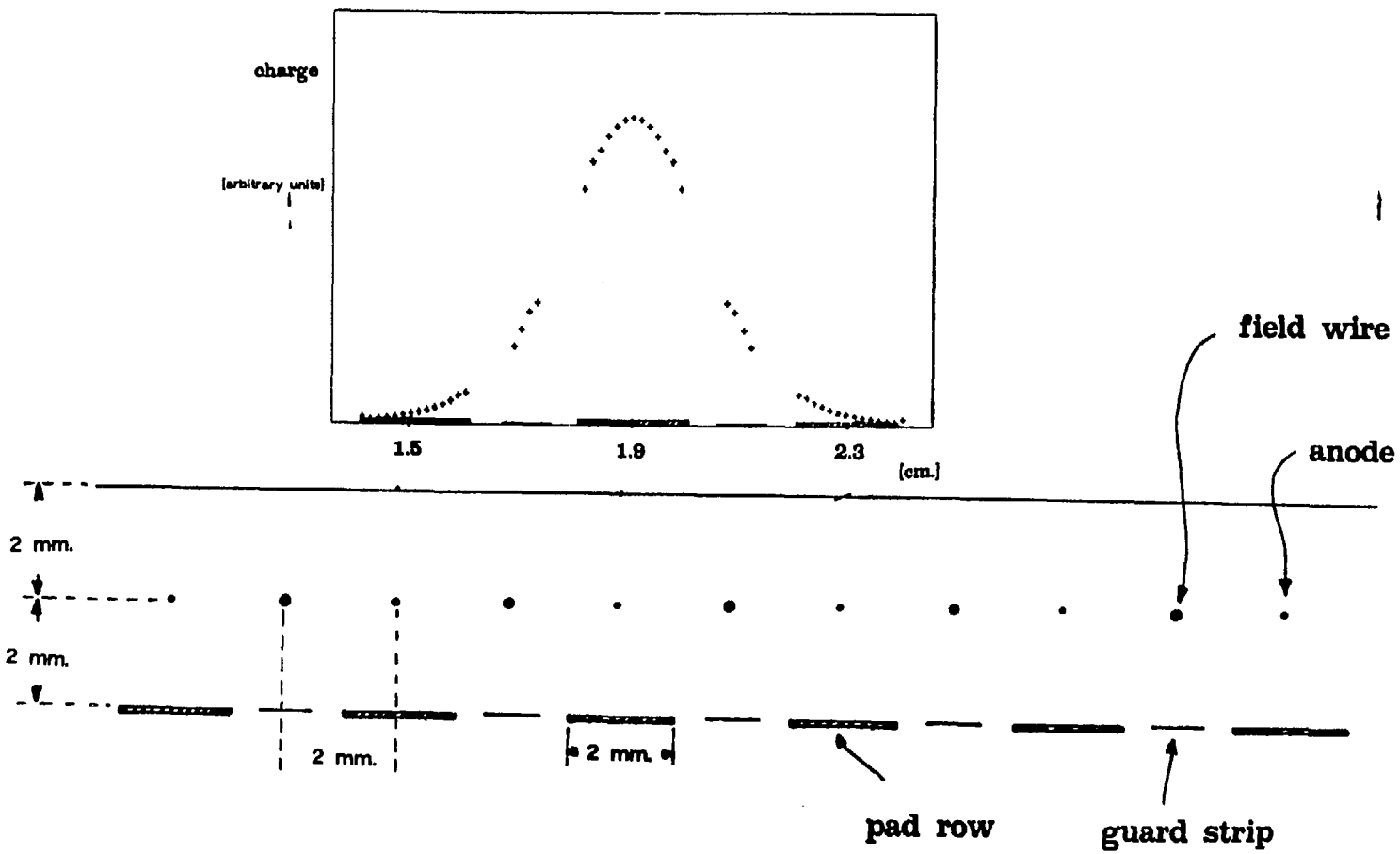

SIDE VIEW

FIG. 1b

Simulated event with 19 hits

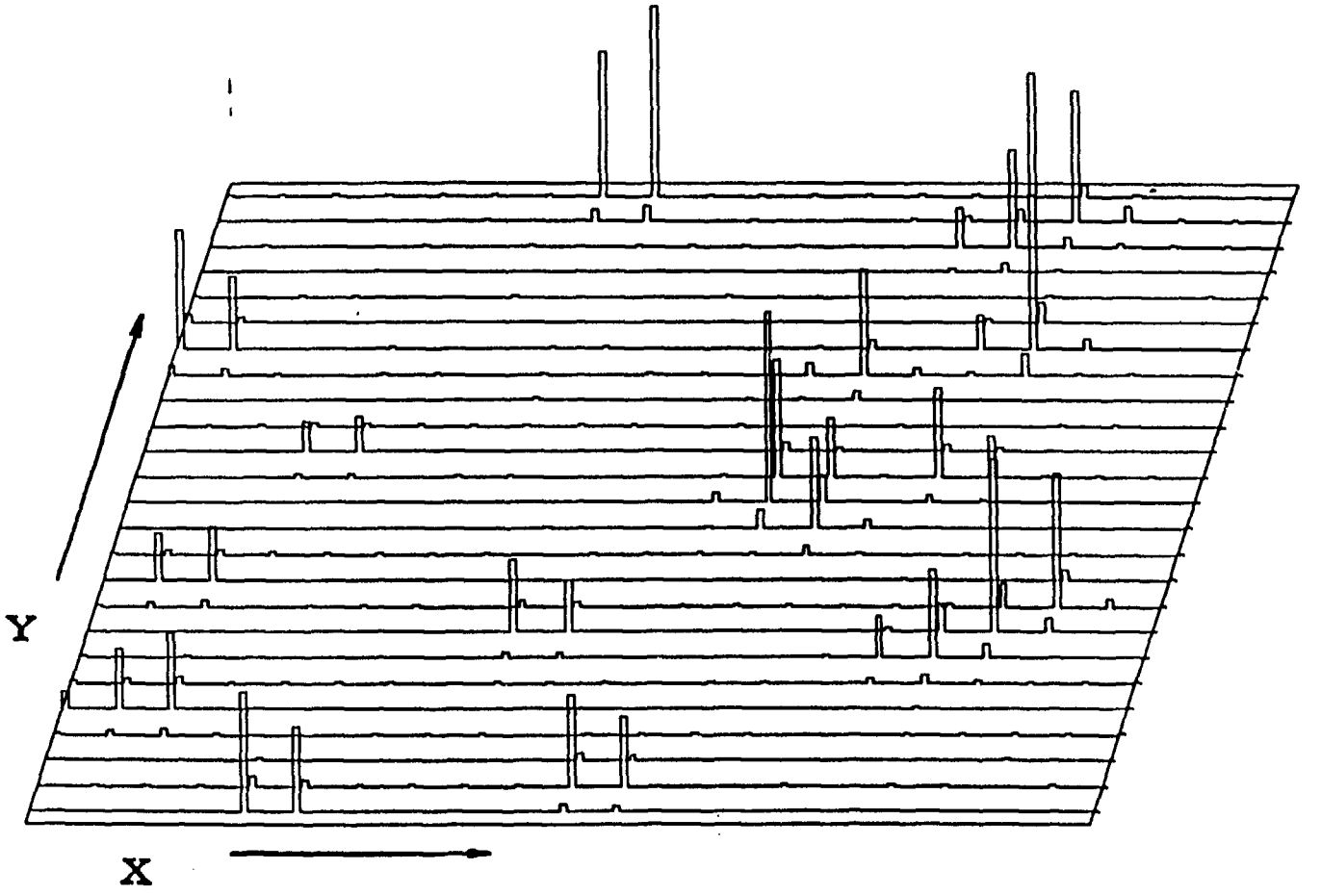

FIGURE 2

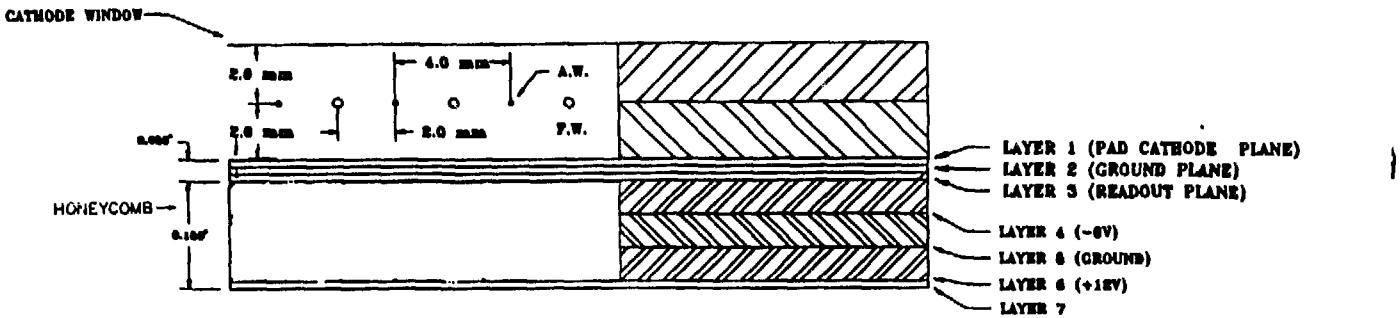

FIGURE 3a

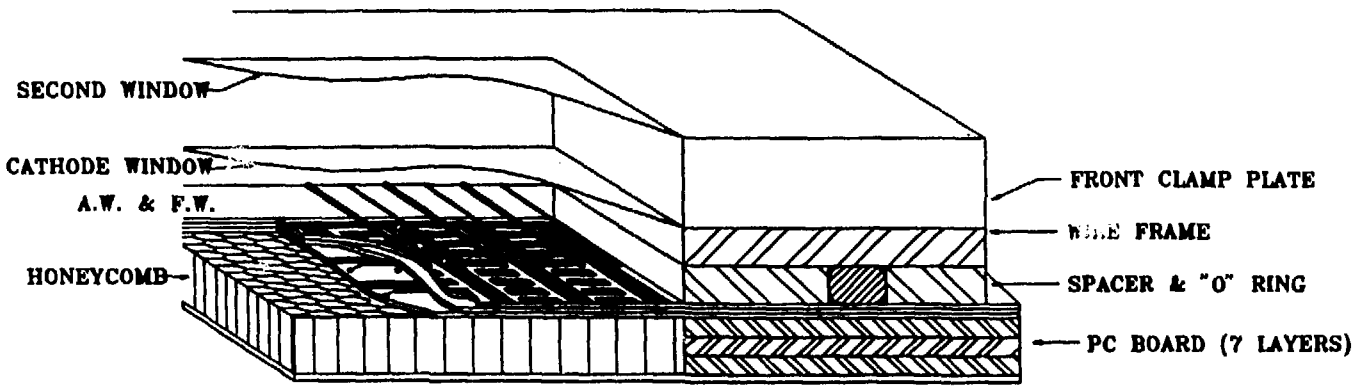

FIGURE 3b

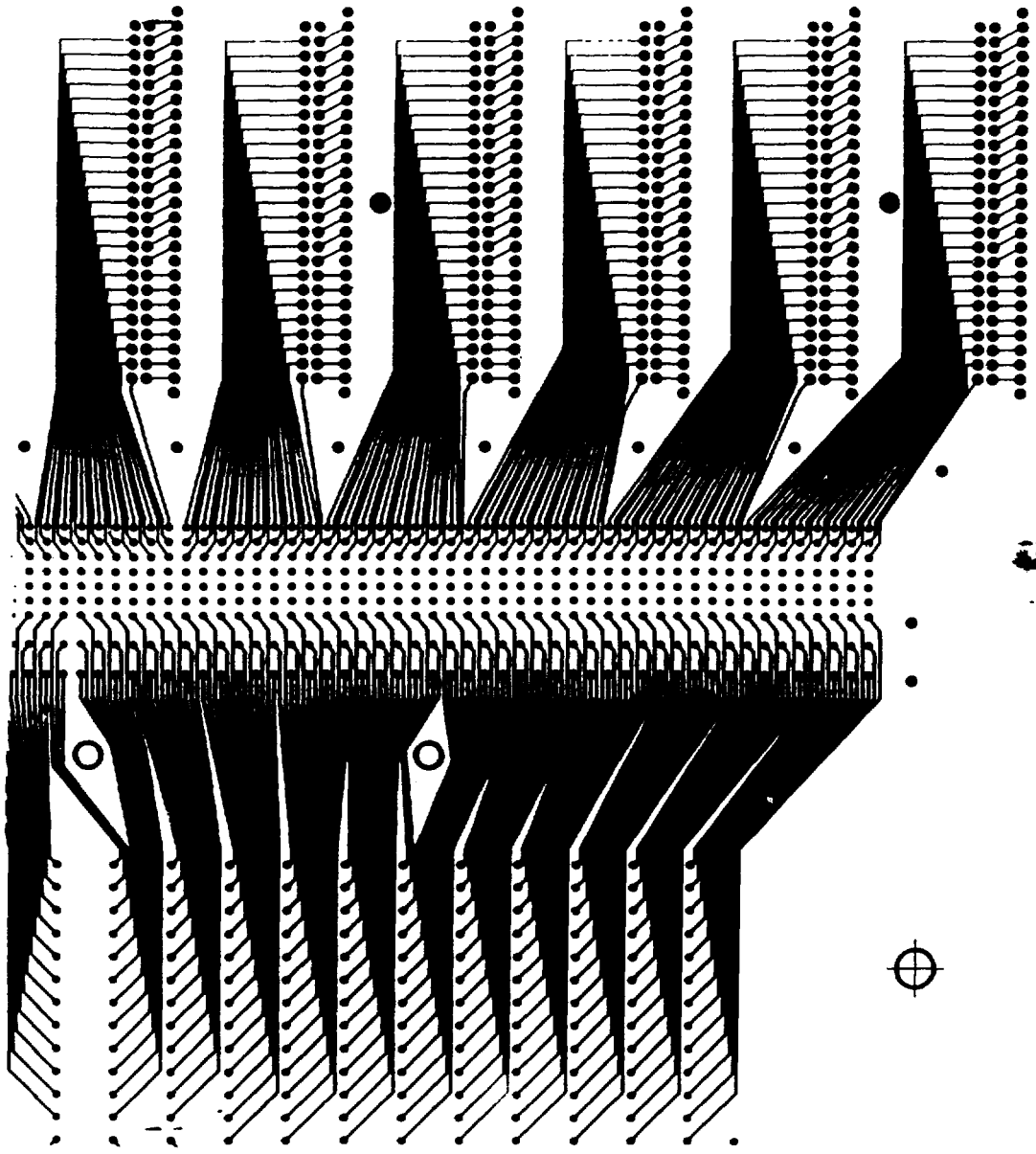

FIGURE 4

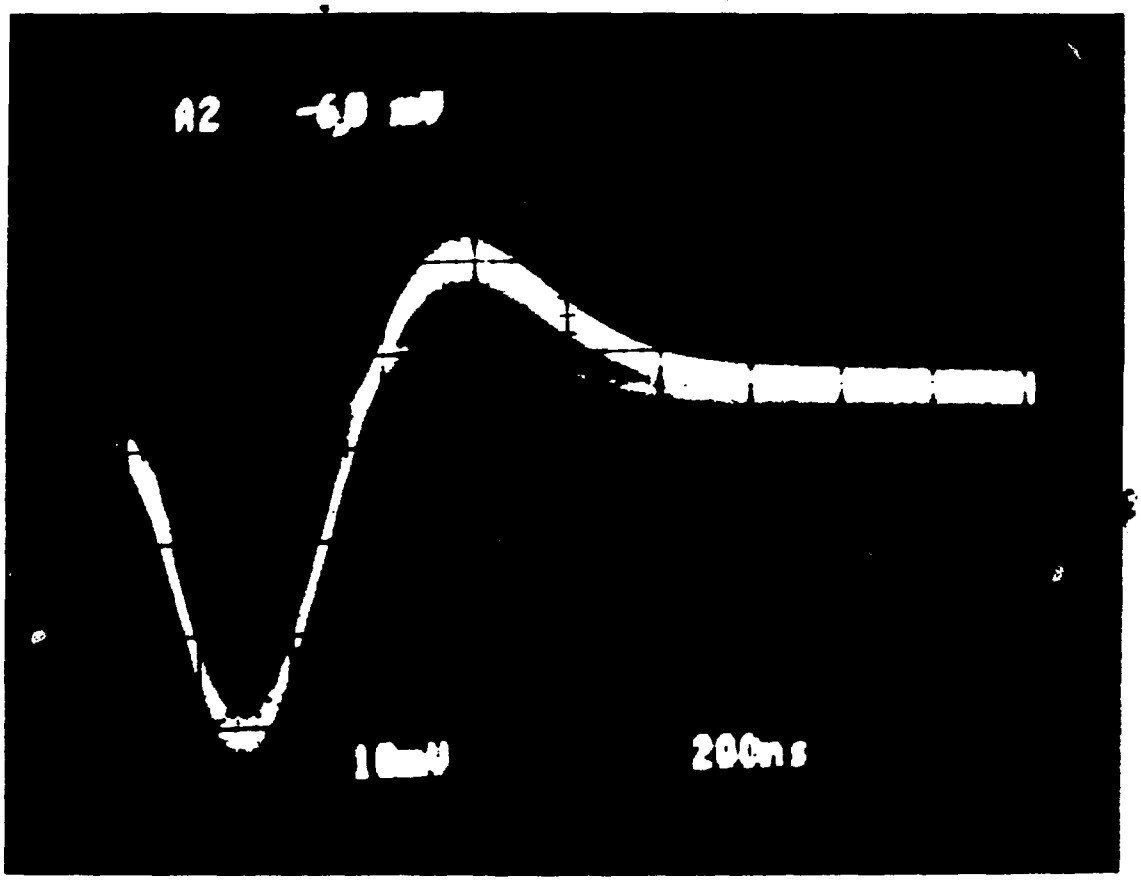

FIGURE 5

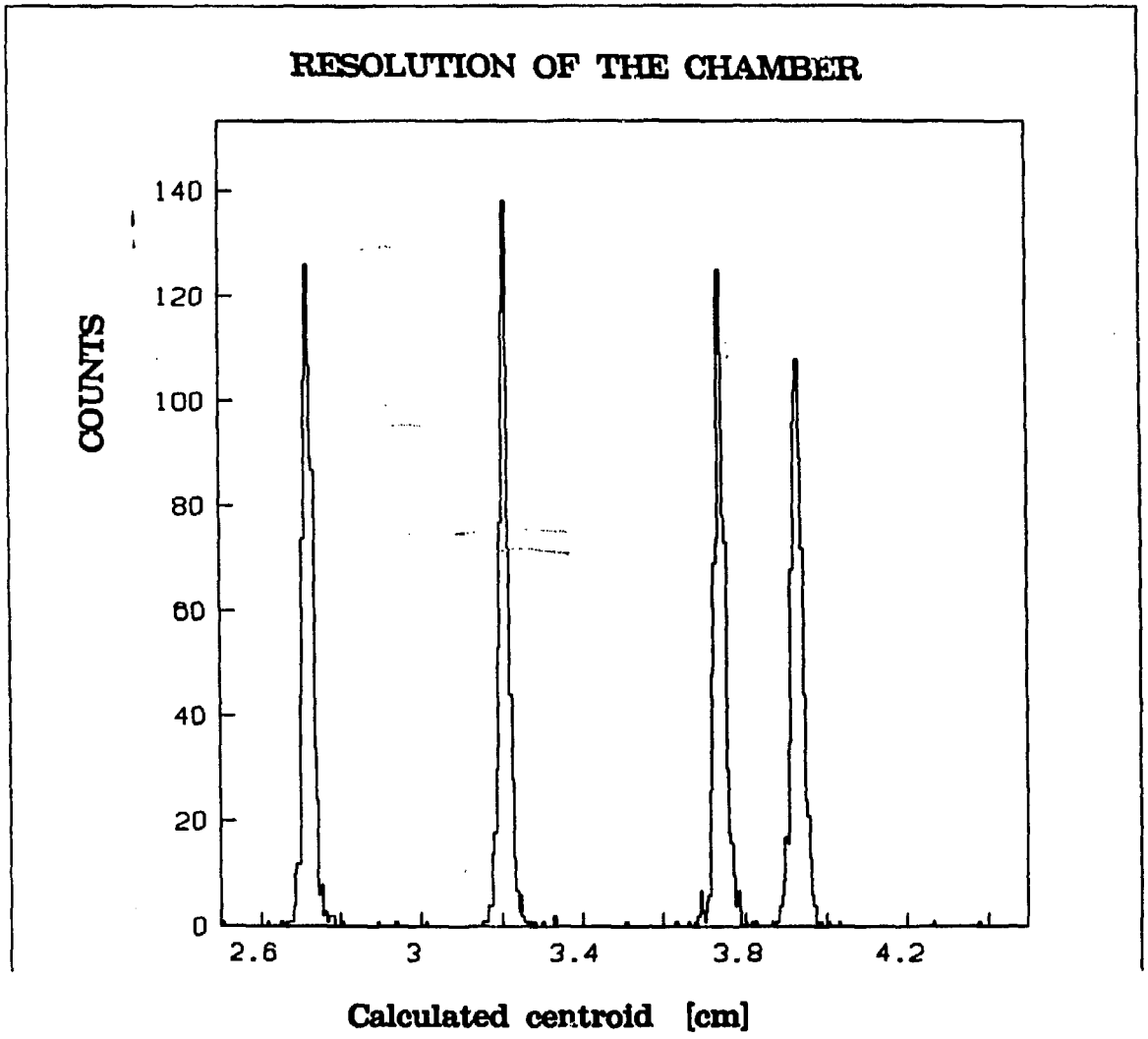
RESOLUTION OF THE CHAMBER
COUNTS
140
120
100
80
60
40
20
0
2.6
3
3.4
3.8
4.2
Calculated centroid [cm]
bin size = 50 microns

FIGURE 6

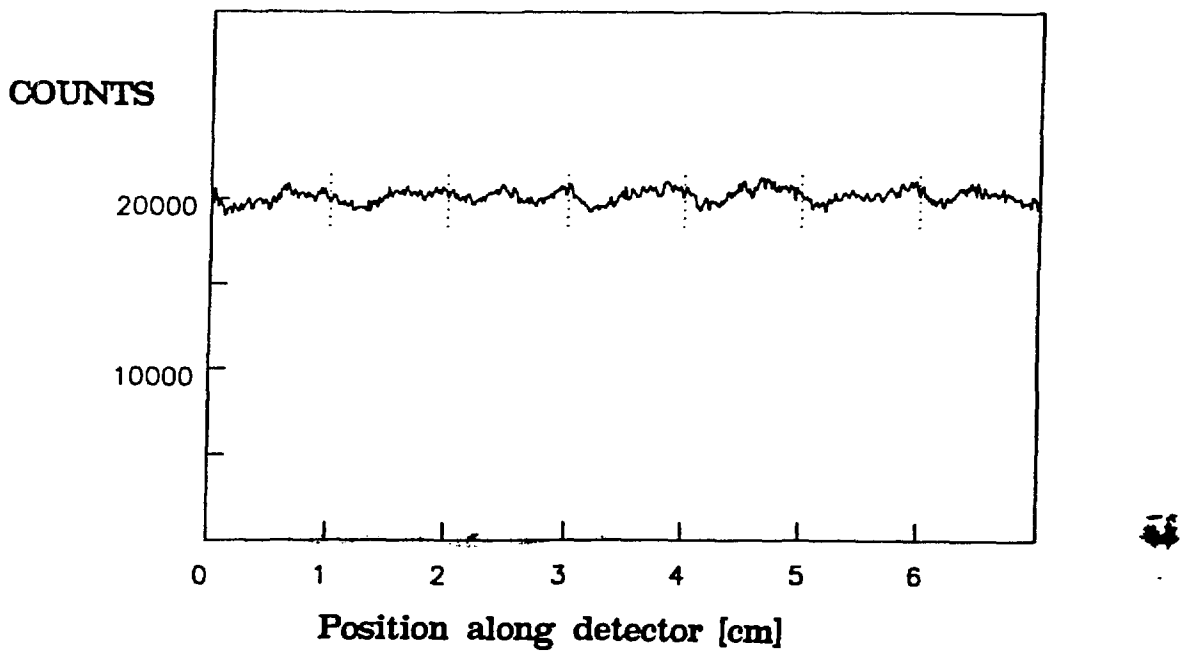

FIGURE 7a

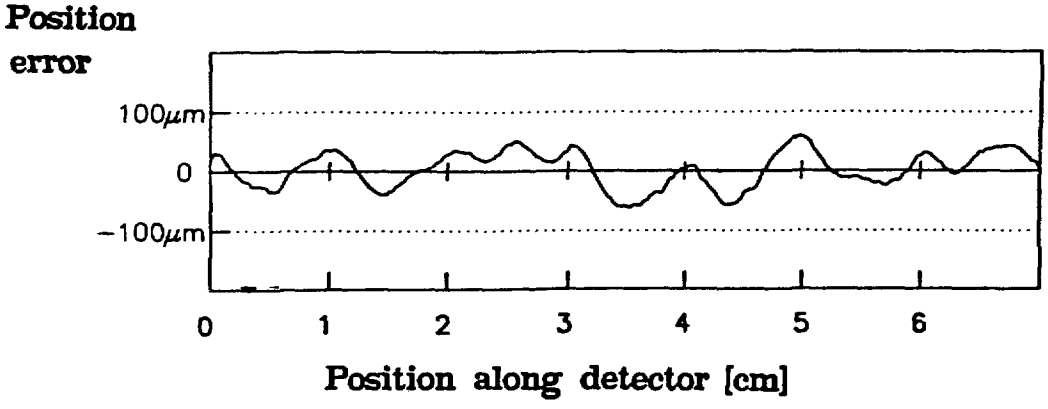

FIGURE 7b

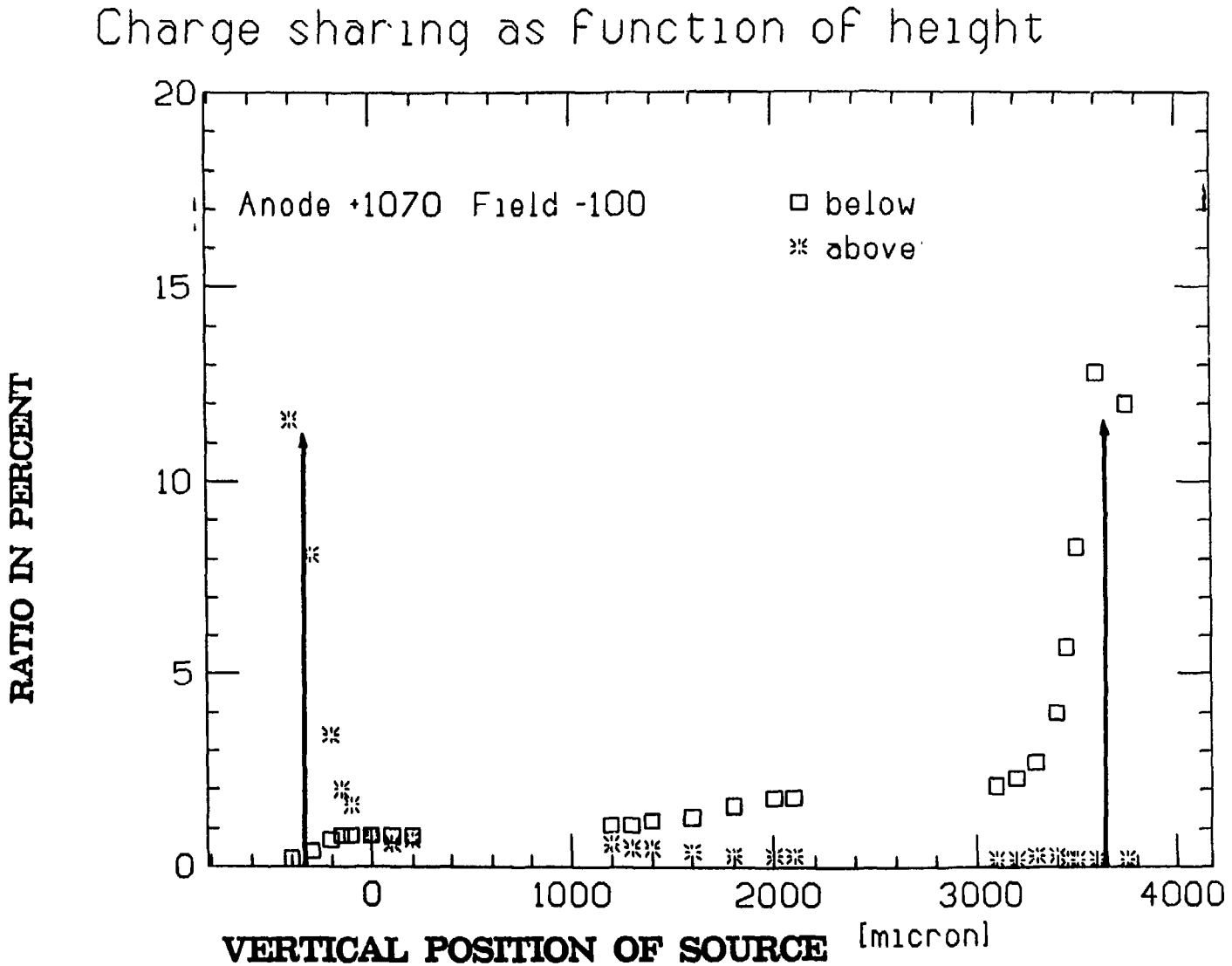
Charge sharing as function of height
Anode +1070 Field -100
below
above
20
15
10
5
0
0
1000
2000
3000
4000
RATIO IN PERCENT
VERTICAL POSITION OF SOURCE [micron]

FIGURE 8

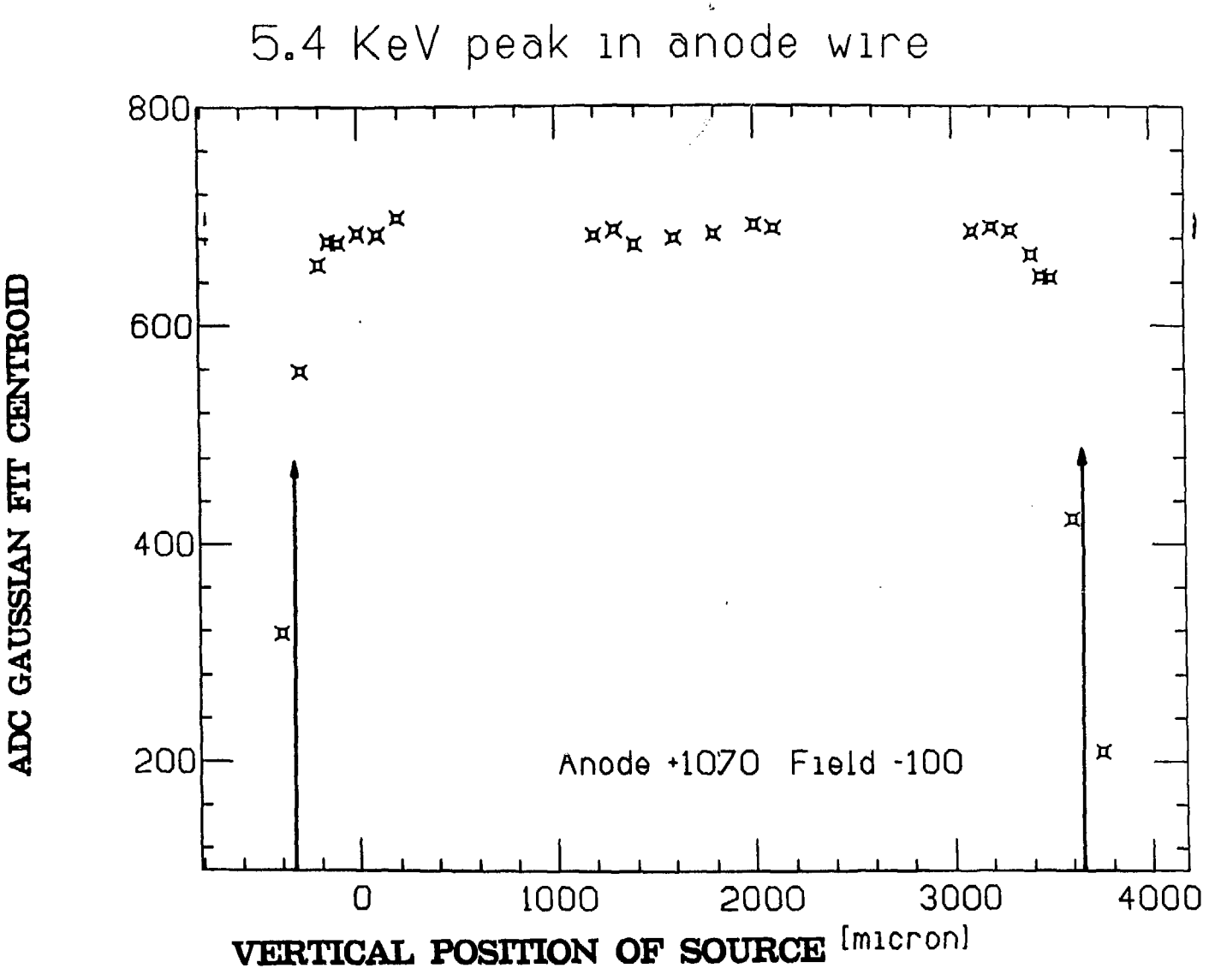
5.4 KeV peak in anode wire
800
600
400
200
Anode +1070 Field -100
0
1000
2000
3000
4000
ADC GAUSSIAN FIT CENTROID
VERTICAL POSITION OF SOURCE [micron]

FIGURE 9